


Article

Design of Guided Bending Bellows Actuators for Soft Hand Function Rehabilitation Gloves

Dehao Duanmu ¹, Xiaojun Wang ¹, Xiaodong Li ^{1,2}, Zheng Wang ³ and Yong Hu ^{1,2,*} 

¹ Department of Orthopedics and Traumatology, LKS Faculty of Medicine, The University of Hong Kong, Hong Kong 999077, China

² Orthopedics and Traumatology, The University of Hong Kong-Shenzhen Hospital, Shenzhen 518000, China

³ Department of Mechanical and Energy Engineering, Southern University of Science and Technology, Shenzhen 518000, China

* Correspondence: yhud@hku.hk

Abstract: This study developed a soft pneumatic glove actuated by elliptical cross-sectional guided bending bellows to augment finger-knuckle rehabilitation for patients with hand dysfunction. The guided bending bellows actuators (GBBAs) are made of thermoplastic elastomer (TPE) materials, demonstrating the necessary air tightness as a pneumatic actuator. The GBBAs could produce different moments of inertia when increasing internal air pressure drives the GBBAs bending along distinct symmetry planes and exhibits anisotropic kinematic bending performance. Actuated by GBBAs, wearable soft rehabilitation gloves can be used for daily rehabilitation training of hand dysfunction to enhance the range of motion of the finger joint. To control each finger of the gloves independently to achieve the function of manipulating gestures, a multi-channel pneumatic control system is designed, and each air circuit is equipped with an air-pressure sensor to make adjustments based on feedback. Compared with general soft robotic exoskeleton gloves currently used for hand dysfunction, the GBBAs actuated soft gloves have the advantage of enhancing the rehabilitation strength, finger movement range, and multi-action coordination applied with guided bending bellows actuators.

Keywords: soft gloves; soft actuator; guided bending; rehabilitation



Citation: Duanmu, D.; Wang, X.; Li, X.; Wang, Z.; Hu, Y. Design of Guided Bending Bellows Actuators for Soft Hand Function Rehabilitation Gloves. *Actuators* **2022**, *11*, 346. <https://doi.org/10.3390/act11120346>

Academic Editors: Yuichi Kurita, Steve Davis and Takayuki Tanaka

Received: 19 October 2022

Accepted: 21 November 2022

Published: 25 November 2022

Publisher's Note: MDPI stays neutral with regard to jurisdictional claims in published maps and institutional affiliations.



Copyright: © 2022 by the authors. Licensee MDPI, Basel, Switzerland. This article is an open access article distributed under the terms and conditions of the Creative Commons Attribution (CC BY) license (<https://creativecommons.org/licenses/by/4.0/>).

1. Introduction

Hands play a significant role in performing activities of daily living (ADL), with the responsibilities of grasping and physical interaction, compared with other motor organs of the body [1]. The hand dysfunction of post-stroke or brain trauma patients is often manifested as flexion spasm, difficulty in extending interphalangeal joints and metacarpophalangeal joints, and loss of active grasping, hand opening, and finger opposition movement. Commonly, clinical physical therapy adopts passive suppression of spasticity to cope with hand dysfunction through the help of therapists by motoring the joints of patients' affected hands [2]. However, the complexity of the hands' structure and the multi-degree-of-freedom (DOF) feature make it difficult to use non-system passive rehabilitation equipment to recover the weak finger flexor and extensor muscles when the training of massive and repetitive finger joint rotation movements is required to improve motor recovery [3,4]. At the same time, due to an increasing number of patients with hand dysfunction in modern society, a limited number of qualified doctors and physiotherapists cannot meet the treatment needs. Equipped with active control system and actuating hardware, exoskeleton robotic rehabilitation devices can provide massive and repetitive customized daily rehabilitation training to enhance the movement of the finger joints of the patients by themselves. Thus, various active exoskeleton robotic rehabilitation devices have been developed in the therapy and research of hand motor impairment to save patients' rehabilitation time and cost [5]. It has been confirmed by experimental studies that active rehabilitation

devices appear in the subdivision of hand motor functional rehabilitation to reduce burden on patients and physical therapists. Compared with passive rehabilitation facilities, active rehabilitation gloves can expand the range of motion and strength of patients' finger joints with the help of external actuators. The above-mentioned active hand-motor-function rehabilitation devices can be roughly divided into desktop rehabilitation systems, which are mainly used in hospital, such as the Haptic Knob [6], and wearable hand exoskeleton, such as the Hand of Hope in Figure 1a [7].

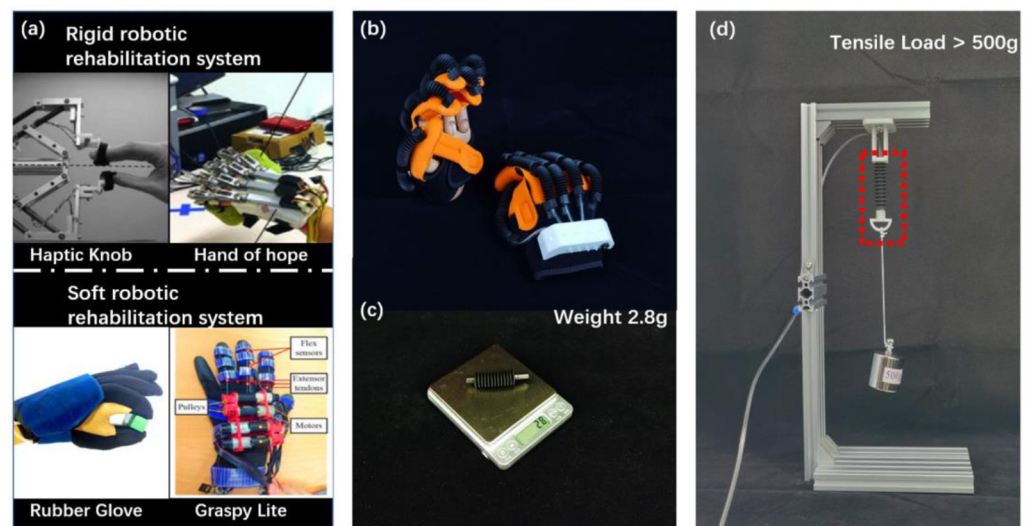


Figure 1. (a) Existing robotic hand dysfunction rehabilitation system; (b) soft exoskeleton rehabilitation gloves actuated by multi-GBBAs; (c) the weight of a single GBBA is 2.8 g; (d) tensile load exceeding 178 times GBBA's own weight.

Regardless of a desktop system or a wearable device, the rehabilitation training with these rigid link structure rehabilitation devices has already been proven effective. However, based on the experience summarized by rehabilitation therapists and doctors using rehabilitation equipment in the treatment of hand dysfunction patients, these rigid active robotic rehabilitation devices still need to be improved to the extent necessary. As far as the hand function rehabilitation robotic system is concerned, the light weight and compactness of the equipment are the most important requirements in addition to sufficient output. In addition, the equipment should be safe and comfortable enough to not interfere with the movement of other joints of the limbs during the patients' wearing for rehabilitation training.

In recent years, engineers have applied soft robotic technology to hand dysfunction rehabilitation devices in the lightweight and human-machine interaction safety problems, such as Rubber Gloves and Grasp Glove using artificial tendons (in Figure 1a) [8,9]. Different from the rigid rehabilitation devices mentioned above, soft robotic rehabilitation equipment is driven by fluid or pull-wire actuators, which make the wearable part softer and more comfortable, especially with fluid-driven soft robots, which have a small output gradient and wide range in dynamics and kinematics, providing multi-feasibility for the development of wearable exoskeleton systems. The advantages of these pieces of rehabilitation equipment in comfort and safety of human-machine interaction can effectively promote the patients' diseased joints to perform massive repetitive flexion and extension rehabilitation in a wide range and help physical therapists to wear these soft devices more conveniently for the patients [10]. However, there are still practical problems for the soft hand-functional rehabilitation equipment, such as insufficient output force and torque, bulky, insufficient robustness, and short service life or limitation of lack of bidirectional output [11]. For the physical rehabilitation of finger knuckles, an ideal external soft actuator

acting on the small single-DOF rotational joints should be miniaturization and enough bidirectional output.

Although the artificial tendons and pull-wire actuators can fulfill the needs of miniaturization and light weight in the application of active wearable hand function rehabilitation equipment, it is hard to meet the requirements of bidirectional output range and force. As for the soft robotic rehabilitation gloves using fluidic elastomer actuators, the main problems are their bulky and insufficient robustness in the flexion of fingers. The design scheme of soft rehabilitation gloves with bellows as the pneumatic actuators has been used by some commercial companies, such as AIREHA and Siyi Intelligence [12,13]. Although the gloves driven by the circular bellows can meet the needs of hand functional rehabilitation to a large extent, the output force of gloves under the same pneumatic system is directly related to the diameter of bellows. Particularly, when such fluidic elastomer actuators are applied to finger joints flexion rehabilitation, the stiffness of the actuators of this size is not enough to provide the pulling force to overcome the grip strength of the finger spasm [14]. Soft pneumatic actuators (SPAs) made of hyper-elastic materials such as silicone rubber or EVA, which deform by changing the fluidic pressure inside the cavity, have a sufficient elongation ratio under small load to drive joint rotation. However, these pneumatic actuators also suffer the defects of insufficient rigidity and out-of-control bending direction when the motion of linear pneumatic actuators through external constraints is converted into bending motion.

We proposed guided bending bellows soft pneumatic actuators (GBBAs) with application in a soft robotic rehabilitation gloves system, providing a large bending angle range and a controllable bidirectional output force for the knuckles and reducing the bulk and mass of the wearable device. GBBAs show a clearly distinguishable output along the long axis and short axis of the elliptical cross-section based on its own structural characteristics. Compared with circular bellows, when the longitudinal diameter of GBBAs remains unchanged, the end output force can be increased by only increasing the length of the major axis, or rather, for the two kinds of bellows with the same end output force, the bulkiness of GBBAs fitted on the gloves is significantly smaller than that of circular bellows, and the bending direction in this case is more suitable for the bending of finger joints. During the experiments and the actual use of soft rehabilitation gloves, GBBAs have provided excellent characteristics in output torque, range-of-motion angles, compactness, and light weight at the state of bending along the short axis of the sectional oval shape when they actuate at the exoskeleton rehabilitation devices of the finger knuckles.

The main contribution of this paper is taking finger-knuckle motion enhancement as an example to provide the design and manufacturing method of soft pneumatic actuators with a guided bending function and bidirectional force and angular displacement output for actuating of soft robotic hand function rehabilitation gloves. The blow molding method of TPE material provides a feasibility of manufacturing GBBAs for the small-size rotary drive used for hand dysfunctional rehabilitation. This processing technology and material enable a GBBA weighing only 2.8 g to withstand a tensile load of more than 500 g to cope with the spasm force that needs to be overcome in the hand function rehabilitation equipment (Figure 1c,d). The transverse section of this kind of soft pneumatic actuator is a flat ellipse, and the cross-sectional moment of inertia around its semi-major axis is much smaller than the semi-minor axis. Thus, it has the characteristic of guiding bending in comparison with the soft pneumatic actuators with a circular cross-sectional profile. Furthermore, due to the different radii of curvature around different rotating shafts, the bending angle of the pneumatic actuators with this flat ellipse cross-sectional profile taking the semi-major axis as the cross-sectional rotating shaft is much larger than that of circular cross-sectional pneumatic actuators with the same effective area. The flat elliptical cross-sectional GBBAs that rely on their different output characteristics bending along different axes, when they bend as the external driver of the rotating joints in the short axis plane, provide a more advantageous output than the circular cross-sectional bellows actuators. As shown in Figure 1c, connecting two or three GBBAs in series as a finger drive device could make full

extension and flexion of the finger knuckles, and then these devices are applied to complete soft wearable hand function rehabilitation gloves.

The following paper will take the finger-knuckles exoskeleton device as the example to describe the design, modeling, experiments and results, and the overall discussion and summary of the guided bending bellows actuators (GBBAs) in each corresponding chapter.

2. Design and Modeling of Guided Bending Bellows Actuators

2.1. Geometric Design

The so-called bellows are known as tubular structures formed by repeating in folding directions of a foldable round table corrugated unit, where segmented cylinders and inscribed cylinders are the wave crests and troughs of the whole bellows, respectively. A complete pneumatic bellows actuator is regarded as the thin wall surface of the truncated cone formed by the connection of wave mountains and valleys, which is made through symmetry and repetition. Therefore, any axial section of the bellows is a complete circle. This kind of circular pneumatic bellows actuator will produce bending deformation with the same effect when subjected to any external force along one direction perpendicular to the central axis [15].

As shown in Figure 2a, when we change the crest and through pattern of the traditional circular bellows from a circle with continuous symmetry to a pattern with a finite number of symmetry axes (such as rectangle or ellipse), the newly obtained pneumatic bellows actuators gain the bending guidance in the plane of their symmetry axis. Due to the various moments of inertia of the cross-section in different directions, the amount of external force required for the bellows to bend to the same angle is also different. The rectangle or elliptical bellows also have two symmetry axes. When the bellows are applied to the rotation joints, they have different performances in different bending directions and simultaneously resolve the stress concentration problem to obtain the required elongation ratio and service life.

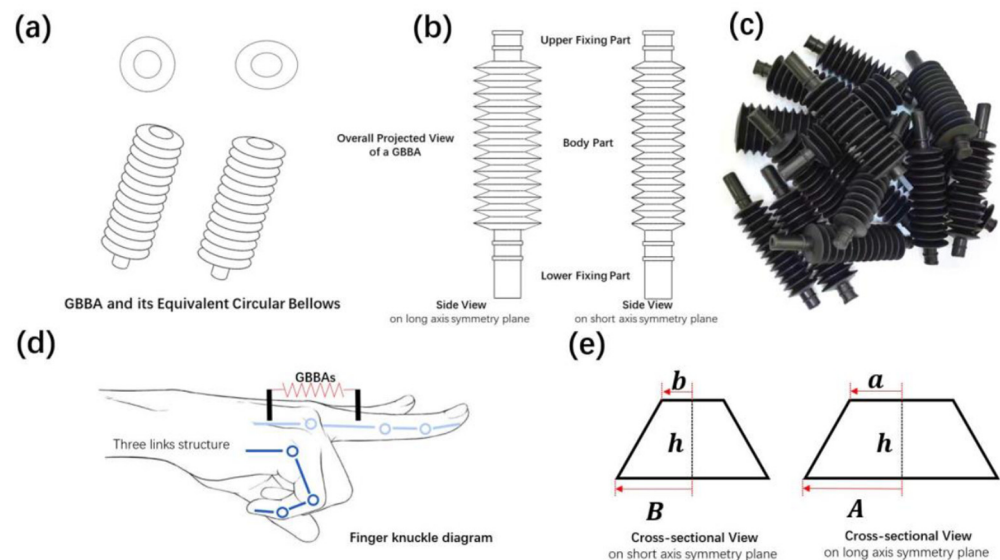


Figure 2. Geometric design of a GBBA: (a) the oval table serves as the minimum folding movement section in a GBBA; (b) comparison of the appearance and structure of the equivalent circular bellows and GBBA; (c) overall appearance of the GBBA; (d) schematic diagram of the working principle of the GBBA; (e) double symmetry planes of the GBBA folding unit.

This elliptical guided bending bellows actuator is composed of a telescopic bellows body part and the upper and lower fixing parts in Figure 2b. In each corrugation, the vertical distance between mountain section and valley section is h , and the entire bellows has $n = 13$ effective corrugations, so its effective overall length is $H = 2nh$, the value of which is like the length of the proximal interphalangeal joint in a relaxed state. As mentioned,

the driving principle of pneumatic bellows comes from the change of corrugation length caused by the internal air pressure. When the actuator is inflated, the internal air pressure is stronger than outside, causing the thin-wall material to stretch and the elongation of the bellows. Correspondingly, when the actuator is deflated, the internal air pressure is lower than outside, resulting in the contraction of the bellows. According to the principle of communicating device in fluidic mechanics, the theoretical end output force F of a GBBA is determined by the internal air pressure and the effective area of the end ellipse:

$$F = \Delta p \cdot \pi AB \quad (1)$$

where A is the length of semi-major axis of crest ellipse, and B is the semi-minor axis.

It is drawn from the long-axis cross-sectional view and the short-axis cross-sectional view of the elliptical GBBA in Figure 2e that the folding angle of the thin-wall structure is different at one wave mountains. When the elliptical GBBA has a length change Δh in one bellow, the angle change at the short axis is

$$\Delta\beta = \tan^{-1} \frac{\Delta b \Delta h}{\Delta b^2 + h(h - \Delta h)} \quad (2)$$

while the angle change at the long axis is

$$\Delta\alpha = \tan^{-1} \frac{\Delta a \Delta h}{\Delta a^2 + h(h - \Delta h)} \quad (3)$$

The dimension design of the elliptical GBBA marked in the cross-sectional view in Figure 2e is listed in the following Table 1:

Table 1. Original design parameters of elliptical GBBA.

Original Design Parameters of Elliptical GBBA		
h	Height of Crest and Trough	3.4 mm
a	Semi-major Axis of Trough Ellipse	4.5 mm
b	Semi-minor Axis of Trough Ellipse	3.5 mm
A	Semi-major Axis of Crest Ellipse	10 mm
B	Semi-minor Axis of Crest Ellipse	8 mm
H	Height of Elliptical Bellows	44.2 mm
t	Thickness of Bellows Shell	0.2 mm

Because the main application of GBBA is for the motion enhancing of the finger knuckles, as shown in Figure 2d, the height of elliptical bellows is determined by the length of a normal finger knuckle.

In the initial state, the folding angles of the corrugations at the semi-major axis and semi-minor axis are, respectively:

$$\alpha = \tan^{-1} \frac{h}{A - a} \quad (4)$$

and

$$\beta = \tan^{-1} \frac{h}{B - b} \quad (5)$$

According to the values given in the table, it can be calculated that the initial folding angle at the semi-minor axis is 36.9° while the angle at the semi-major axis is 31.7° . Therefore, the folding angle of GBBA along the semi-minor axis is larger than the bending along the semi-major axis.

The selection of geometric parameters in the design of the elliptical bellows mainly affects its expansion and contraction ability, the size of the output force, and the bending performance in different directions. The application scenario of the elliptical bellows mainly

acts on the rotation drive of the finger joints; therefore, it must satisfy the needs of the rotation and expansion along the rotation axis of the finger joints and provide sufficient bidirectional output force. When the control system provides the same pressure source as the power system, the maximum elliptical section of GBBAs is used as the effective output area, providing the required stress.

2.2. Manufacturing

Various methods such as additive manufacturing and demolding processing can be used to produce air-tight pneumatic soft actuators [16,17]. To ensure GBBAs have sufficient expansion ratio and proper rigidity in their dimension, the suitable wall thickness is about 0.2 mm. Current additive manufacturing methods for processing soft actuators cannot meet the wall thickness requirements in the design due to insufficient resolution of the printer. Thus, we choose the way of mold forming to manufacture GBBAs, such as injection molding and blow molding [18,19]. Even if these actuators should be processed by demolding methods, there are diverse flexible materials and corresponding processing technologies available. It is required to select appropriate processing methods and materials based on multiple factors such as the pressure-bearing capacity and dimensional size accommodated with soft actuators.

The following requirements of materials and processing techniques are necessary in the main application in hand dysfunctional rehabilitation of the GBBAs. As an external driving device for the finger joints, the weight of the GBBAs should be as small as possible to reduce the burden on the wearers, and they should be soft enough to avoid secondary damage to the wearer's affected hand. In terms of materials and structural properties, there are also two points that must be paid attention to when choosing GBBAs' processing technology. Most importantly, the selected flexible material should satisfy the design requirements mentioned above, can realize the corresponding expansion and cuts, and have sufficient bearing capacity. Another point is that as a flexible structure that can be used in the medical field, it must meet the needs of service life and large-scale mass production. Therefore, some small-mass molding processes cannot be applied in this design, such as the popular additive manufacturing technology.

Based on the requirements, it is essential to select a suitable processing technology and material to produce GBBAs with thin wall thickness, non-circular cross-section, strong pressure-bearing capacity, long service life, and mass production. The blow molding thermoforming processing method using TPE (Thermoplastic Rubber) molecules as the processing raw material provides the feasibility for the manufacture of GBBAs. We choose black TPE (Thermo-Plastic-Elastomer) materials as the raw material for blow molding of GBBAs in the production line of Ningbo East Plastic Pipe Co., Ltd. The selected TPE materials, also called TPR (Thermo-Plastic-Rubber) materials, are different from the EVA material used for blow-molding corrugated pipes in that they have thin wall thickness and the flexibility required for folding. In addition, the flexible materials in other positions must ensure that the GBBA still maintains its own rigidity to resist finger spasm force instability under the condition of more than 17 N of tension. The black bellows in Figure 2c are GBBAs made in one batch by TPE blow molding. GBBAs processed by TPE can obtain a bellows structure with small weight, thin wall thickness, and sufficient rigidity.

2.3. Modeling

The working principle of the guided bending bellows actuators' displacement is essentially that by changing the air pressure in the cavity, the thin-walled structure produces a pressure difference between the inside and the outside [20], which results in the cumulative displacement of each section of the conical surface (Figure 3c). Through the simulation software Abaqus, the deformation results of the thin-walled structure can be simulated when the inner cavity of the GBBA is filled with different values of air pressure. Using the FEA simulation method to analyze the actuator's driving condition before the formal die opening processing can effectively save the processing cost and time. In Figure 3b, we

simulated the internal air pressure of the actuator to be 120 kPa and 80 kPa, respectively, to determine whether the designed non-isotropic structure would be unstable during a stroke.

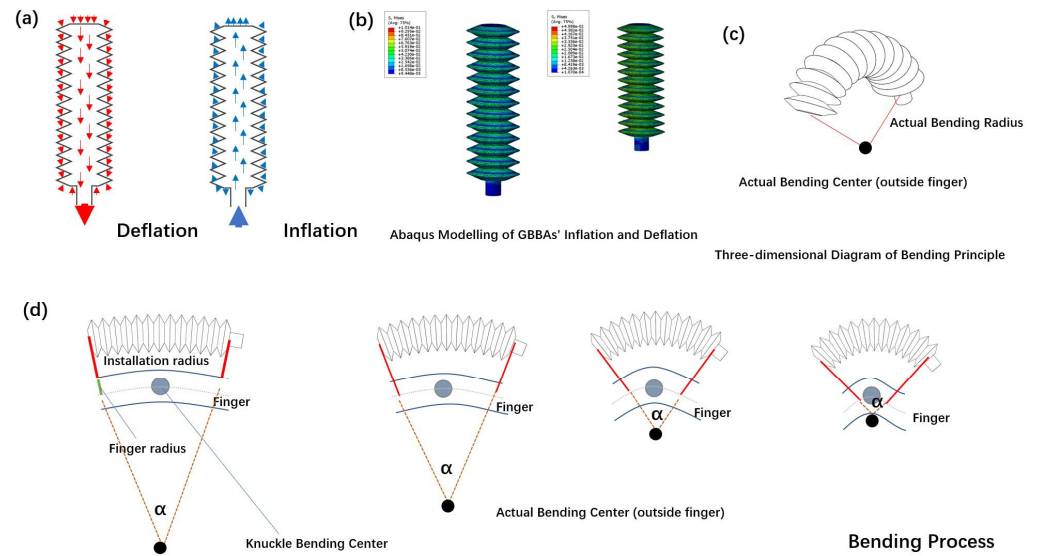


Figure 3. (a) Pressure on the thin-walled structure of the GBBA during inflation and deflation; (b) Abaqus modeling of the GBBA's inflation and deflation under the pressure of 20 kPa; (c) bending principle of the GBBA acting on a finger knuckle; (d) bending process of the GBBA acting on a finger knuckle.

Since the structure of GBBAs is composed of corrugations, the output force and displacement are also the set of the output of each corrugation. When the two ends of the actuator are constrained, the superposition of forces generated by the deformation of the conical surface will eventually act on the end surface. For circular bellows and GBBA with the same number of layers n , if the same static effect is produced, it is necessary:

$$\Delta F_g = \sum_n \Delta p \cdot S_g \tag{6}$$

$$\Delta F_c = \sum_n \Delta p \cdot S_c \tag{7}$$

Since the projections of the bellows and GBBAs on each layer are constant circles and ellipses,

$$\pi ab = \pi r^2 \tag{8}$$

According to the design parameters of the GBBA, it is inferred that the radii of the crest and trough of the circular bellows with equivalent mechanical effect are 7.94 mm and 3.97 mm, respectively. As the actuating structure in a soft robotic exoskeleton system, the flat actuators are smaller in size and more compact in structure compared to the circular actuators.

The bending movement of the knuckle driven by GBBAs comes from the torque converted by the axial force by constraining the relative distance and vertical angle between the two ends of the actuators and the bending center of the knuckles, as shown in Figure 3c,d. The two ends of the GBBA are always perpendicular to the surface of the finger during the bending of the knuckle [21], and the actuators are bent uniformly in the finger's bending direction. Therefore, the moment arm of the bending process is also a constant value in each section:

$$R = R_I + R_F \tag{9}$$

where R_I and R_F are the installation radius and the finger radius, respectively. It is known that both lengths of the knuckles are l . Thus, the torque during bending is:

$$M = 2 \int_0^{\frac{\alpha}{2}} f \left(R + \frac{l}{\tan \frac{\alpha}{2}} \right) \tag{10}$$

Combined with the output of the axial force of the GBBA:

$$M = \Delta p \cdot S_e \cdot \left(R_I + R_F + \frac{l}{\tan \frac{\alpha}{2}} \right) \tag{11}$$

Through experiments, the effective area of the actuator’s axial force output can be measured, and the torque acting on the knuckles at any bending position can be obtained from the above-mentioned mechanical model. Clinical practice could significantly benefit from controlled force accurately on the joints during rehabilitation through changing the internal air pressure of the actuator.

3. Experiments on Single GBBA

The rehabilitation of finger joints is mainly to exercise tendons and finger muscles through repeated bending and stretching of the finger joints, stimulate motor nerves, and promote blood circulation in the fingers to achieve the effect of relieving or even curing spasms [22]. As mentioned above, GBBAs are external drives designed to cope with this knuckle rehabilitation scene. The mechanical model of the knuckles can be simplified as a two-link with a single DOF rotating around a kinematic pair and only one DOF rotational movement (Figure 4a) [23]. When GBBA act on the knuckles, the force output along the central axis will be converted into the torque of the finger rotation, and the amount of expansion and contraction produced along the central axis will be converted into the angular displacement of the finger rotation.

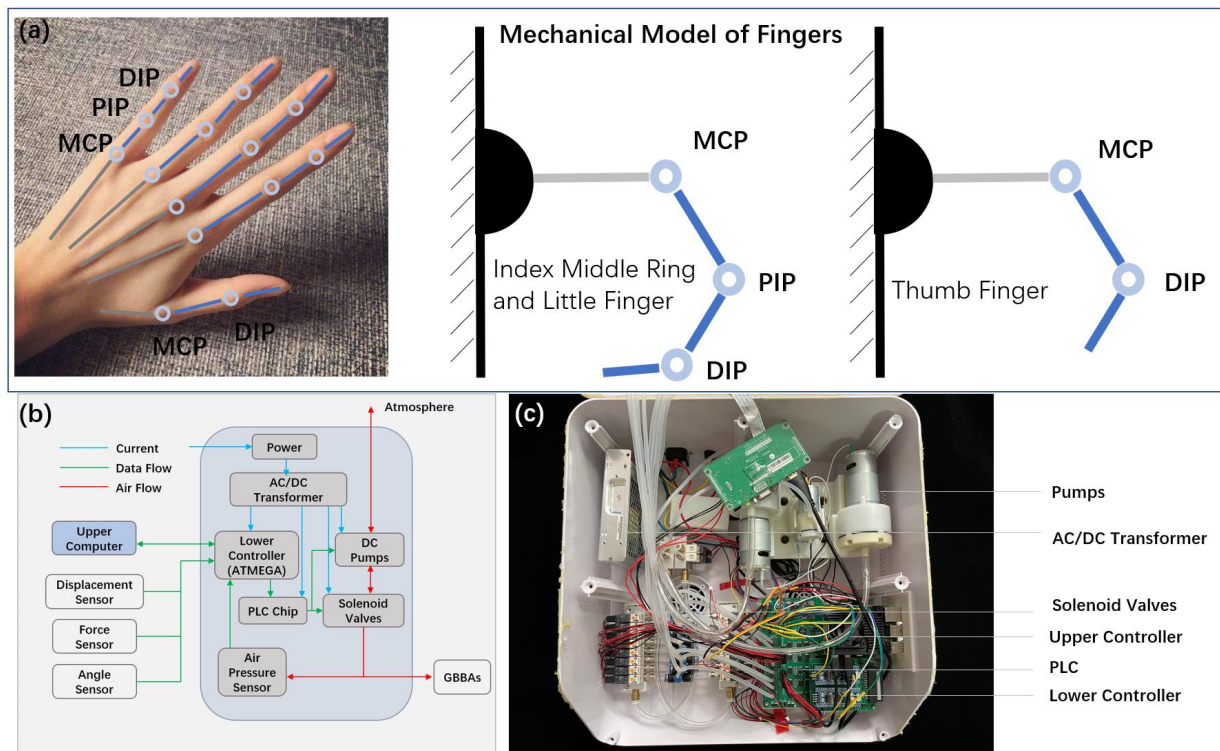


Figure 4. (a) Mechanical model of fingers rotation in one hand; (b) schematic diagram of control system which concludes current flow, data flow, and air flow; (c) physical diagram of the corresponding ten fingers control box.

Since the initial structure of GBBAs produced by blow molding has no bending deformation, this kind of actuator has the characteristic of linear motion without restriction. Therefore, the mechanical and kinematic performance of GBBAs can be evaluated in linear motion. In the linear motion test, the relationship between the output force, displacement, and internal air pressure of the actuator can be detected intuitively, which has a guiding role for the micro-motion control of the GBBAs applied on the rotary. Another significance of our design of linear motion is that the different joints of different people's fingers have great discrepancy in size, so the same rehabilitation equipment applied on patients' hands will have varied performance. In the final analysis, the rotary motion of the knuckles comes from the constraint transformation of the linear motion of the actuators in a specific bending direction. Thence, the linear motion performance experiments are more universal than others for the evaluation of pneumatic soft actuators. Simultaneously, to intuitively obtain the relationship between the internal air pressure of the GBBAs and the bending angle of the knuckles driven by them, we have designed a bionic knuckle-bending experiment that constrains both ends of the GBBAs.

3.1. Control System

Although we have designed various experiments to test the output performance of GBBAs under different conditions, all of these experimental platforms use the same control system (shown in Figure 4b). The routes of the entire control system include a green information route, blue electric circuit route, and red gas route, which represent the control signals, electric energy, and gas flow direction in the system correspondingly. Figure 4c shows the lower controller and gas drive system of the physical diagram based on the three routes' schematic diagram.

In the open-loop control system, the control signals are sent from the upper computer to the lower controller (ATMEGA328P-AU) through the serial port for processing [24]. Then, the analog signals processed by the lower controller are sent to the PLC drive chip (Macrowis, 4 WAYS) to pneumatic components such as drive pumps (Chaofer, ES-3910, DC24V) and solenoid valves (OST Solenoid 2/2 NC, 24 V). The signals collected in the system are directly sent to the lower controller by the air-pressure sensor, laser displacement sensor, force sensor, and angle sensor. The electrical energy of the system is converted from AC power to 24 V DC power by the power supply (JC Power, 24 V 72 W), which supplies to the PLC chip module, DC pumps, and solenoid valves. The compressed or vacuum gas from the compression and vacuum pump is transferred to the main gas route through two parallel solenoid valves. After the solenoid valves, there is a manual flow valve to control the flow rate in the gas circuit to remain stable. Ultimately, the control instructions issued by the upper computer are executed as compressed or vacuum gas passing into GBBAs under the cooperation of the modules in the control system.

3.2. Linear Experiments of Pneumatic Bellows Actuators

The torque and angle displacement required for finger joint rehabilitation come from the axial output force and displacement of GBBAs [25]. Thus, the purpose of the linear motion test is to standardize the input parameters and output performance of GBBA so that it can be used as the pneumatic soft actuators of soft robotic exoskeleton gloves.

3.2.1. Internal Air-Pressure and Output Displacement Performance

The displacement output of GBBAs along the central axis is constrained by the knuckle joints and converted into angular displacement around the central shaft of the knuckle joints, and the elongation of GBBAs is converted into a circular arc along the orbit above the knuckles. To obtain sufficient bending of the fingers wearing rehabilitation gloves equipped with GBBAs, the elongation ratio of these actuators must meet the requirements of the movement of the driving position of the device. Ideally, the two ends of GBBAs remain perpendicular to the fingers during the bending stroke, and the entire actuator is evenly stretched. According to the size of the connecting device and the radius of the bionic

finger-knuckle shaft, it can be calculated that the ultimate compression length of GBBA should be less than 45 mm and should be greater than 60 mm to achieve 90° bending of knuckle joints.

The working principle of GBBA relies on the change of internal air pressure, causing the folding angle between the corrugations sections to change, thereby generating displacement in the direction of the central axis [26]. We have built a linear motion displacement monitoring platform to measure the relationship between the input air pressure and the output displacement of a GBBA without external load. The intake end of the GBBA is fixed on the aluminum alloy base by a 3D-printed bracket, connected by an air pipe with the air source through the hollow bracket (shown in Figure 5a). Each side of the bracket is connected to a slide rail parallel to the central axis of the GBBA, whose slider is fixed on both sides of the 3D-printed top cap. At the same time, the sealing end of the GBBA is fixed at the center of the top cap, so that its linear movement can only be along the direction of the central axis. The two parallel slide rails provide lateral support to the tested actuator to prevent the test results from being interfered with by lateral forces. Furthermore, the entire base device is placed horizontally to prevent the GBBA from being affected by its own weight during linear motion. This set of devices can ensure that the movement of the GBBA to be measured is strictly in the direction of the central axis and will not be deformed due to lateral forces such as gravity, and the test results of the output force do not need to be superimposed on the gravity factor.

We use a laser displacement sensor (HG C1400, Panasonic, Osaka, Japan) and pressure sensor (XGZP6847A, CF Sensor, Wuhu, China) accordingly to measure the motion state and the internal air pressure of the tested GBBA. This laser displacement sensor is fixed on the cantilever at the other end of the base, and the measuring beam is shot at the center of the top cap of the actuator at a frequency of 50 Hz, that is, the measuring point located on the top cap instead of the GBBA itself. The air-pressure sensor is in the air circuit and records the internal air pressure of GBBA in real time and also at a frequency of 50 Hz.

3.2.2. Internal Air-Pressure and Output Force Performance

The force detection requires that the force sensor and the actuator are always in full contact [27], which is different from the platform that measures the displacement output. As shown in Figure 5b, the intake end of the GBBA is also fixed on a 3D-printed bracket which is connected to the aluminum alloy base and connected to the air-source system through a PVC pipe. The air pressure sensor in the system can record the pressure at a frequency of 50 Hz inside the actuator in real time. Similarly, a connecting top cap is connected to the sealed end of the GBBA to be tested, and on the opposite side of this top cap a force sensor (DYLY-103, DAYSENSOR, Bengbu, China) is fixed. Like displacement measurement, the force sensor is fixed on the cantilever at the base, which is adjusted to the right position, keeping the actuator original length. In this experimental platform, hot melt glue is used to connect the end of the actuator and 3D-printed bracket while screw bolts are used to connect the force sensor, brackets, and base to prevent fluctuations in the reading of the contact sensor.

The acquisition frequency of the force sensor is the same as the acquisition frequency of displacement at 50 Hz. During the whole experiment, we should keep the length of the tested GBBA at the original length without changing. When negative air pressure is applied to the actuator, that is, when the actuator is deflated, the output force is shown as tension, and the reading of the force sensor is negative; when positive air pressure is applied to the actuator, that is, when the actuator is inflated, the output force is shown as thrust, and the reading of the force sensor is positive. The negative and positive values of the force sensor only present the direction of the force, not the magnitude.

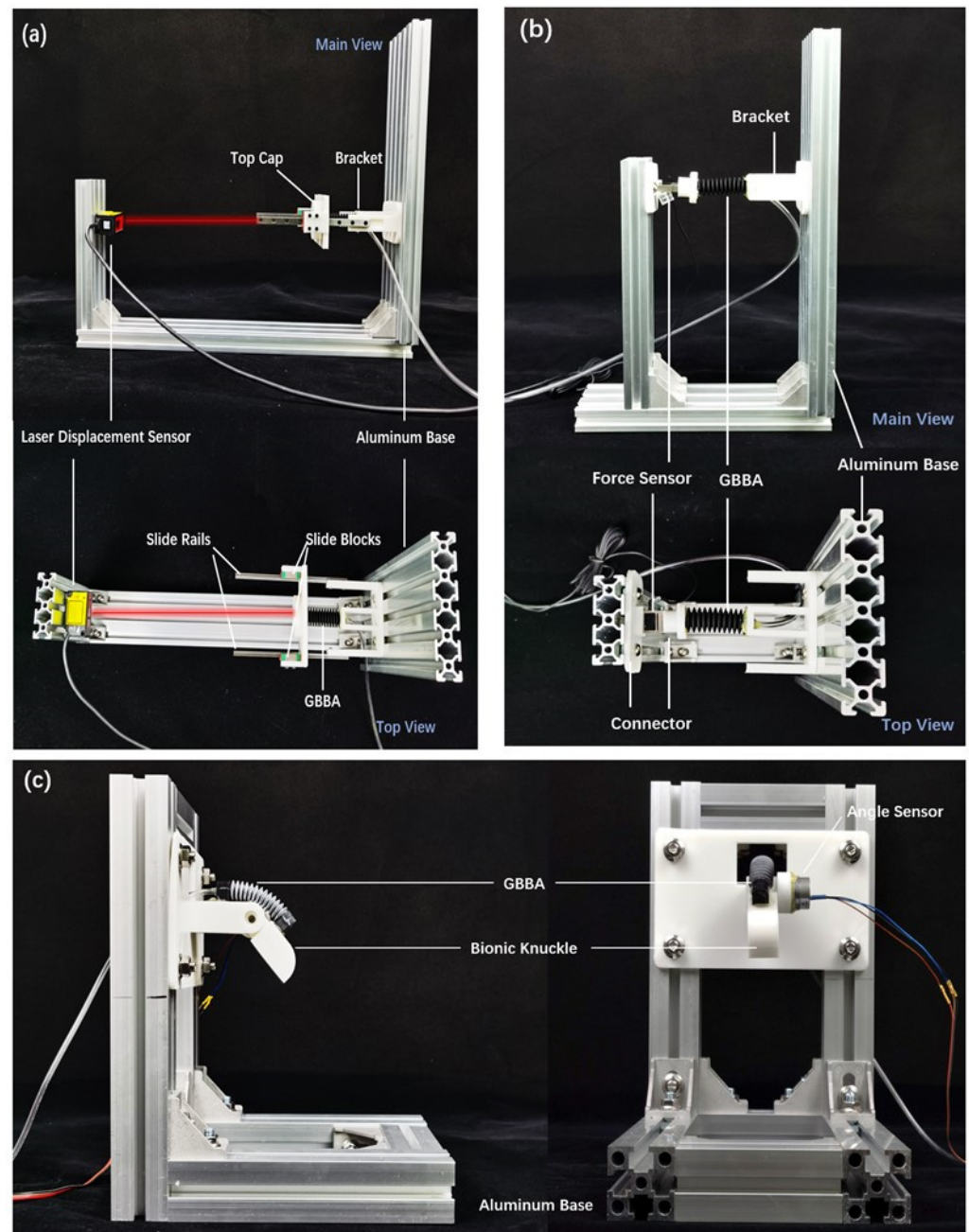


Figure 5. Experiments of a single GBBA: (a) output displacement experiment; (b) output force experiment; (c) bending experiment of single GBBA acting on a non-damping bionic finger joint.

3.3. Bending Experiments of Pneumatic Bellows Actuators

The ultimate application purpose of GBBA is to drive the rotational motion of the finger joints through converting the linear motion into a rotational motion with only one DOF constrained by the rotation motion pair and the connectors on the two end faces of the actuator. Therefore, the relationship between the internal air pressure of GBBA and the bending angle of rotation joints is also a significant experiment content. For this purpose, we designed bionic knuckles as the objects to be tested in the bending experiments.

A universally sized bionic knuckle was designed to simulate the effect of GBBA acting on finger joints of approximate dimensions due to the differences in the size of the hands of people of different body types and the joints of different fingers of the same hand. The width of this bionic knuckle is 20 mm, the length is 30 mm, and the bending radius is 10 mm, the numerical value of which is similar to that of the middle finger's mid-end

joint of an adult male. After assembling the two sections of the bionic knuckle through the shaft, when one section is fixed, the other can rotate smoothly around the shaft to achieve joint bending. In the bending experiment of a single knuckle, we use an angle sensor (WXXY, GTB, 5V-180, Millay, Taizhou, China) to measure the rotation angle of the joint. In addition to measuring the rotation angle of the knuckle, the angle sensor also acts as an undamped joint rotation axis to avoid the influence of the frictional force during rotation on the experimental results.

In Figure 5c, the proximal bionic knuckle is fixed on the aluminum alloy base, facing the horizontal direction, while the distal bionic knuckle is connected with the proximal through a rotating shaft, which enables the distal knuckle to rotate freely around the shaft in the vertical plane. On one side of the rotating shaft, the installation position of the angle sensor is reversed, and the sensor relates to the fixed section of the bionic knuckle without relative movement. The rotation angle test shaft of the sensor relates to the rotating section of the bionic knuckle, keeping the angle synchronized with it. The intake end surface of the GBBA is vertically connected to the fixed section of bionic knuckle through the connecting pieces, while the sealed end's surface is vertically connected to the rotating section of the bionic knuckle through other connecting pieces. When positive or negative pressure gas is passed into the tested GBBA, the length of this actuator is changed, pushing or pulling the rotating section of the bionic knuckle to rotate around the shaft. GBBA should be installed on the testing bionic knuckle along the semi-short axis symmetry plane and semi-long axis symmetry plane, respectively, and bending output data in these two directions can be obtained. It is important to note that to drive the bionic knuckle bending in the different symmetry planes of the GBBA, it is necessary to change the installation direction of the actuator and the connecting pieces, and at the same time, the distance between the central axis of the actuator and the upper surface of the bionic knuckle must be kept the same.

3.4. Buckling and Guided Bending Comparison

Compared with EVA material, the most important feature of TPE bellows is that it can blow out corrugations with a larger ratio of wave crest to wave trough. Coupled with the larger elastic modulus of the material itself, the soft actuator has more stable structure. We stretch the traditional EVA circular bellows and TPE GBBA to the same elongation ratio and then deflate the air to the same air pressure, -50 kPa, to observe the degree of structural damage (Figure 6, left).

The thin-walled structure of the EVA circular bellows has been severely buckled, but the structure of GBBA could remain. Similarly, to verify the bending guidance of the elliptical cross-section bellows structure, we compressed the EVA circular bellows and the GBBA to the same ratio, inflated into the same positive pressure, and observed its bending without external force interference (Figure 6, right).

As expected, the isotropy of the circular actuator makes its bending direction uncontrollable [28], while the elliptical cross-section actuator instinctively bends along the direction of the minimum moment of inertia, that is, the plane of the minor axis due to different moments of inertia. Although the isotropic structure has advantages in installation convenience and adaptability, the elliptical cross-section GBBA has more obvious guidance in the preset bending direction.

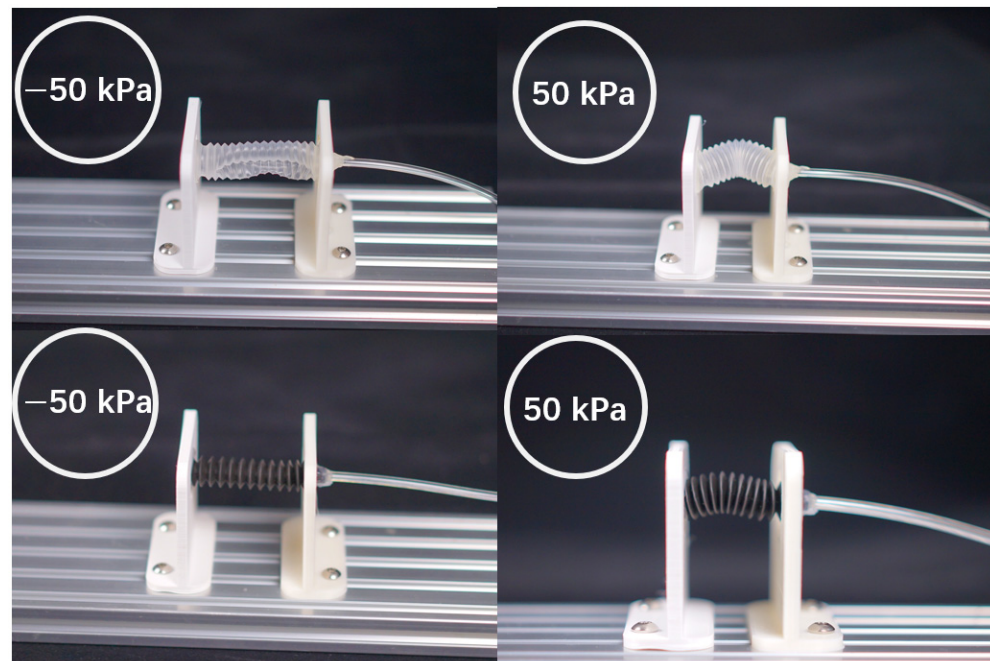


Figure 6. Comparison of EVA circular bellows and TPE GBBA: stretched to the same ratio for structural stability tests with the same deflation or compression ratio.

4. Result

In the linear experiment of a single GBBA, we selected the relationship between internal air pressure and displacement during inflation and deflating to analyze its displacement performance and hysteresis as a pneumatic soft actuator and the relationship between air pressure and output force to verify the model's performance correctness [29]. While in the bending experiment of a single actuator, we verified its bending guidance by comparing the angle output of the same actuator along different axes.

4.1. Results in Linear Experiments

The experimental results of internal air pressure and output displacement of a GBBA under compress and extend motions are plotted in Figure 7a, where the abscissa and ordinate are the absolute value of the internal air pressure and the relative value of the displacement of the end surface of the GBBA, respectively. In the curves, the difference of the maximum value and minimum value of the GBBAs' displacement from the extreme y coordinate presents the linear deformation. Combined with the original length of the GBBA, it can be seen that the elongation ratio is more than two hundred percent. Comparing Figure 7a, during extension and contraction GBBAs show significant hysteresis, which mainly exists between the initial 40 kPa and 80 kPa during the inflation process and between the initial 220 kPa and 160 kPa in the deflation process. The hysteresis of GBBAs means that when they are applied to the soft robotic hand functional rehabilitation gloves, the flexion and extension time of the fingers are not symmetrical. Figure 7b displays a time curve of output displacement over a complete cycle, where the internal air pressure varies linearly with time. Predictably, the extension time of the actuator is much less than the compression time.

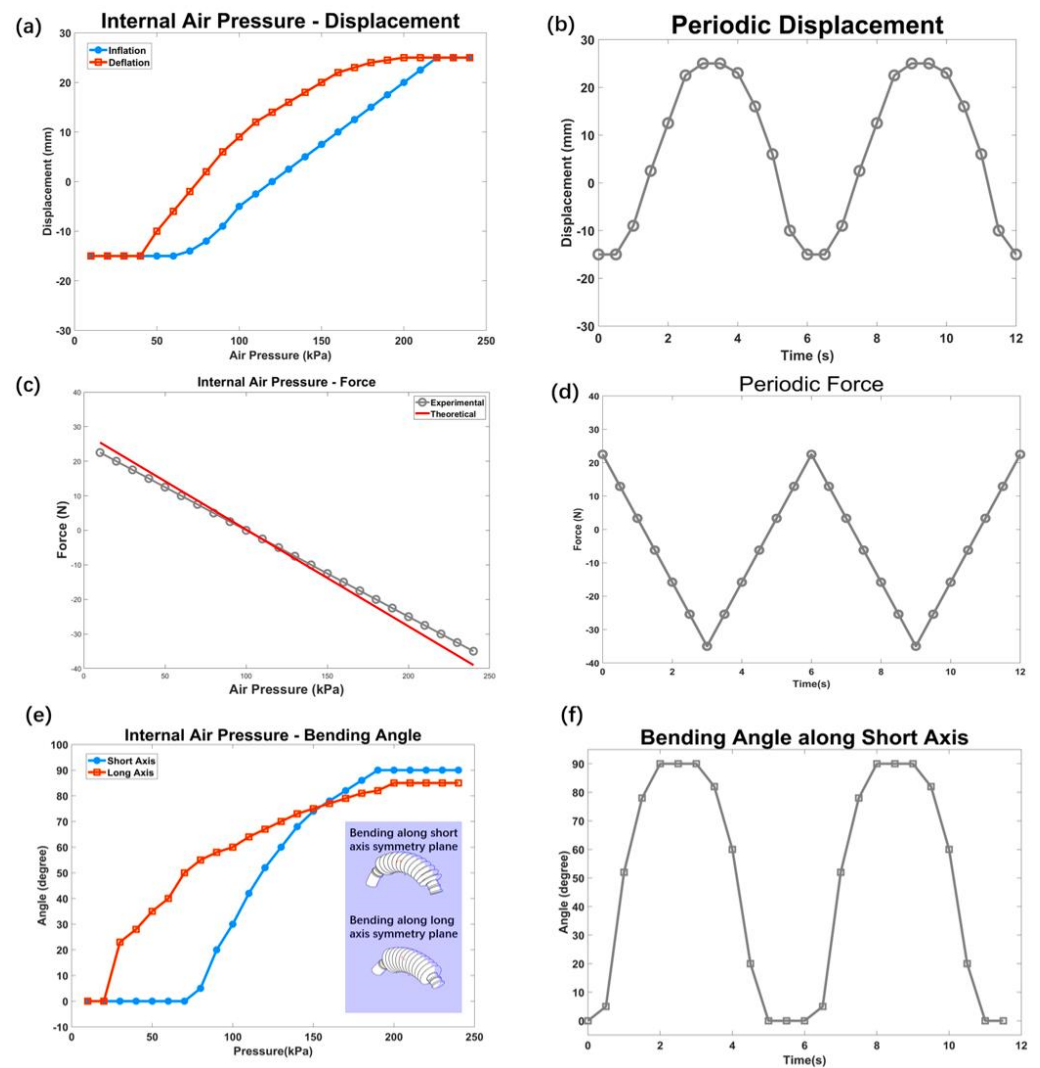


Figure 7. Results' curves. (a) Hysteresis curves: relationship between the internal air pressure and output displacement during inflation and deflation; (b) periodic displacement curve: output displacement in two cycles; (c) relationship between the internal air pressure and output force; (d) periodic force curve: output force in two cycles; (e) bending angle curves: relationship between internal air pressure and bending angle along short- and long-axis symmetry plane; (f) periodic bending angle curve: bending angle along short axis symmetry plane.

Under the original length of the GBBA, the relationship between internal air pressure and output axial forces is plotted in Figure 7c, where the abscissa and ordinate of the curves present the absolute value of the internal pressure and the absolute value of the output axial force, respectively. Accordingly, the theoretical values of the internal air pressure and output force of the GBBAs are also plotted in Figure 7c. The slope of the curve, that is, the theoretical effective output area, is basically consistent with the actual situation. In addition, it must be noted in the curves that the sign of the vertical axis indicated the direction of the force, not the magnitude. The experimental results are compared with the weight of the GBBA itself, whether the thrust or pulling force reaches hundreds of times its own weight. When the internal air pressure varies uniformly with time, the output force as a function of time is shown in Figure 7d. The maximum and minimum values of the air pressure are 10 kPa and 240 kPa, respectively, with a 6 s cycle time.

To meet the needs of hand cramp rehabilitation, the maximum internal negative pressure inside GBBAs should be 20 kPa according to the maximum pulling force of one

spasm finger, which is about 17 N. Based on the experimental results, the outputs of the GBBA under valid operating conditions are listed out in the following Table 2:

Table 2. Maximum input and output characteristics of the GBBA measured in linear experiments.

	Value
Input negative pressure	20 kPa
Input positive pressure	240 kPa
Elongation	25 mm
Compression	−15 mm
Elongation ratio	90.4%
Output thrust	35 N
Output tension	25 N

Table 2 lists all the maximum input and output parameters of the GBBA measured in these linear experiments.

As the finger joint can be regarded as one single-degree-of-freedom rotating link structure, the output torque of the GBBA could be calculated from the linear experimental results. Assuming that the radius of bending of the finger joint is 10 mm, the torque within the effective air-pressure range can be calculated:

$$M_{max} = F_{max} \cdot (l_f + l_c) \quad (12)$$

where M_{max} is the maximum output torque calculated from the maximum output force F_{max} , while l_f and l_c are the bending radius of the finger joints and the installation distance between the central axis of the GBBA and the finger surface. Substituting the measured data from the experiment, the theoretical values of the maximum external torque of flexion and extension when the joints are driven by GBBA are 0.35 Nm and 0.25 Nm, which could satisfy the requirement of finger-knuckle rehabilitation.

4.2. Results in Bending Experiments

As mentioned above, the GBBA has two axes of symmetry and produce different bending outputs along these symmetry planes. The diagram in Figure 7e depicts the two states of the GBBA bending along the short- and long-axis symmetry planes. The data curves of the internal air pressure of the GBBA and the bionic knuckle angle along the short-axis symmetry plane and the long-axis symmetry plane are plotted in Figure 7e. Based on the angle of the bionic joint in the straight state as zero degrees, with the increasing of the air pressure inside the GBBA, this bionic knuckle gradually bends, and the value of the angle increases.

It can be drawn from comparison that whether it is a flexing or straightening process, the bending angle range in the short axis plane can reach 90°, while the bending angle range in the long axis plane is only 50°. In the device driven by GBBA along the short-axis symmetry plane, when the internal air pressure is less than 80 kPa, the bending angle of the knuckle is a stable 0°. While in the device driven by GBBA along the long-axis symmetry plane, it is not enough to straighten the bionic knuckle even when the internal air pressure is 40 kPa. In the no-load state, the GBBA-driven device along the short-axis symmetry plane not only has a larger output bending angle, but the required input air pressure variation range is also smaller than that of the device driven along the long-axis symmetry plane. According to the bending modeling, the difference in torque output along different axes' symmetry planes comes from the difference in force and bending radius [30]. Therefore, for the bellows actuator with elliptical cross-sectional structure, the output bending angle and torque in short-axis symmetry directions show significant differences.

From the results of linear experiments, the relationship between the output force and the internal air pressure is a linear function. However, the nondamping single-knuckle-bending experiment tells that the effective internal air-pressure limits are from 80 kPa to

190 kPa. To avoid tension unable to reach what is required during hand rehabilitation, we set the air-pressure range of each cycle to 20 ~ 240 kPa, and each cycle lasts 6 s. In Figure 7f, the curve is a function of the knuckle angle and time. In one cycle, the knuckles stay at the fully flexion and extension position to ensure sufficient torque.

5. Development of Soft Rehabilitation Gloves

Similar to the knuckle joint, the structure of one finger can be simplified to a simple three-link device. Then, we can treat the rehabilitation of hand function by soft robotic gloves as three GBAs in series driving the three-link structure flexion or extension. Thus, we have designed a bionic finger to verify the motion-enhancing effect of the soft rehabilitation gloves acting on a single three-joint finger. The size of this bionic finger is the same of that of the bionic knuckle, except for the addition of a fingertip joint, whose numerical value of the size also comes from the middle finger of an adult man [31]. The three sections of the bionic finger are connected by two shafts and can rotate freely between each other.

For the bending of a total finger, we are concerned about the angle of fingertip rotation, not the relative angle of each of the two sections [32], so we did not use the same angle sensor measurement method as in the bionic knuckle rotation experiment but used an IMU sensor (Risym, GY-85, Shenzhen, China) to read the angle change of the fingertip section during the process of flexion or extension. In Figure 8a, from the side view of the bionic finger-bending experiment, the three-linked GBA rehabilitation device is assembled on the finger, and the angle of the finger is about 270 degrees (the angle parallel to the end finger section is zero) in the initial state, where the internal air pressure of this three-linked device is the same as the outside air pressure. When high-pressure air is inflated into this rehabilitation three-linked GBA, the bellows elongate and drive the bionic fingers to flex. Correspondingly, the extension of the bionic finger comes from the contraction of the bellows caused by the deflation of the three-linked GBAs device.

The photos of the bionic finger from the initial state to the flexion and extension state are shown in Figure 8a,b, where the blue dotted lines indicate the rotational position of each knuckle. The internal air pressure and bending angle curve measured of one cycle by the experimental platform are plotted in Figure 8c, in which as the internal pressure of the finger rises from 77 kPa to 160 kPa, the fingertip has rotated more than 250°. At the maximum input air pressure, this GBAs Glove can drive fingers to make a full fist, while the minimum straighten angle is 20° because of the small length of DIP joint. With a cycle of 6 s, when the internal air pressure changes from 20 kPa to 240 kPa, the three-dimensional coordinate curve of time, air pressure, and bending angle can be drawn as shown in Figure 8d.

To avoid relative sliding between the GBA series and the finger, we need a glove base with sufficient elasticity as the connection medium between the driving devices and the fingers, which can be worn on the hand without sliding relative to the skin of the hand at the process of flexion and extension and can also be bonded to the connecting pieces of the driving devices [33,34]. As shown in Figure 9a, the dark gloves are elastic intermediate gloves made of neoprene (SBR CR), which are comfortable and easy to wear and have enough wrapping properties to prevent fingers from sliding inside the gloves during flexion and extension.

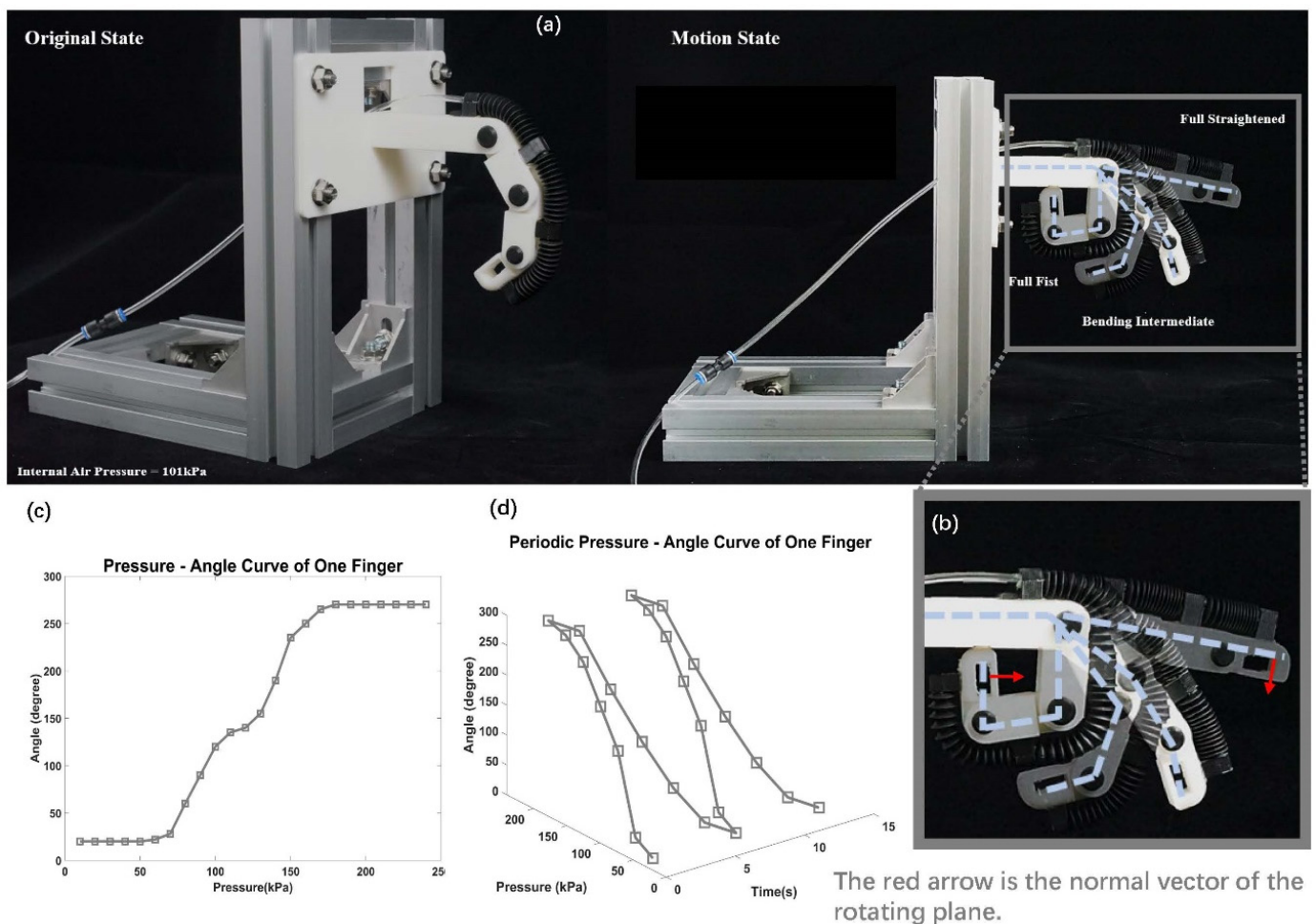


Figure 8. Motion of the bionic finger driven by the three-linked GBBAs. (a) Original state and motion process of the bionic finger from full straightened to full fist; (b) the IMU sensor collects the normal vector of the fingertip angle during movement; (c) fitting curve of fingertip angle of bionic finger with internal air pressure; (d) periodic bending angle curve with air pressure: relationship between bending angle and internal air pressure in two cycles.

There are two types pneumatic driving devices used in this soft exoskeleton glove, namely, the two-linked GBBAs acting on the thumb and little finger and the three-linked GBBAs acting on the middle three fingers, which depends on the length of the fingers. The design idea of the driving device is to connect multiple GBBAs in series in the same gas channel to realize common movement during the process of flexion and extension. The inside of the GBBAs' connection to the driving devices is a 4 mm diameter air pipe made of PVE, which is sealed by an arched connector, whose bottom is the bonding position of the neoprene gloves.

The soft exoskeleton gloves' control device has a total of five different air channels, which control the flexion and extension of the five fingers [35]. Thus, the driving devices of each finger can be individually controlled so that after the gloves are worn, a variety of gestures can be performed during the rehabilitation training process to exercise different muscles. Some gestures driven by the soft exoskeleton glove are shown in Figure 9b. For example, the index finger and thumb flex, and the remaining three fingers extend to form an "OK" gesture; the index and middle finger extend and the remaining three fingers flex to form a "V" gesture; and a fist or open-hand gestures. In some physical therapy programs for stroked hands or spastic hands, it is necessary to perform repetitive flexion and extension training on one or several fingers to stimulate a specific muscle group [36], thereby helping the corresponding neurological rehabilitation in turns. These five-channel

soft rehabilitation gloves can meet the requirement of driving any fingers to bend and extend repetitively according to the needs of the physical therapy program.

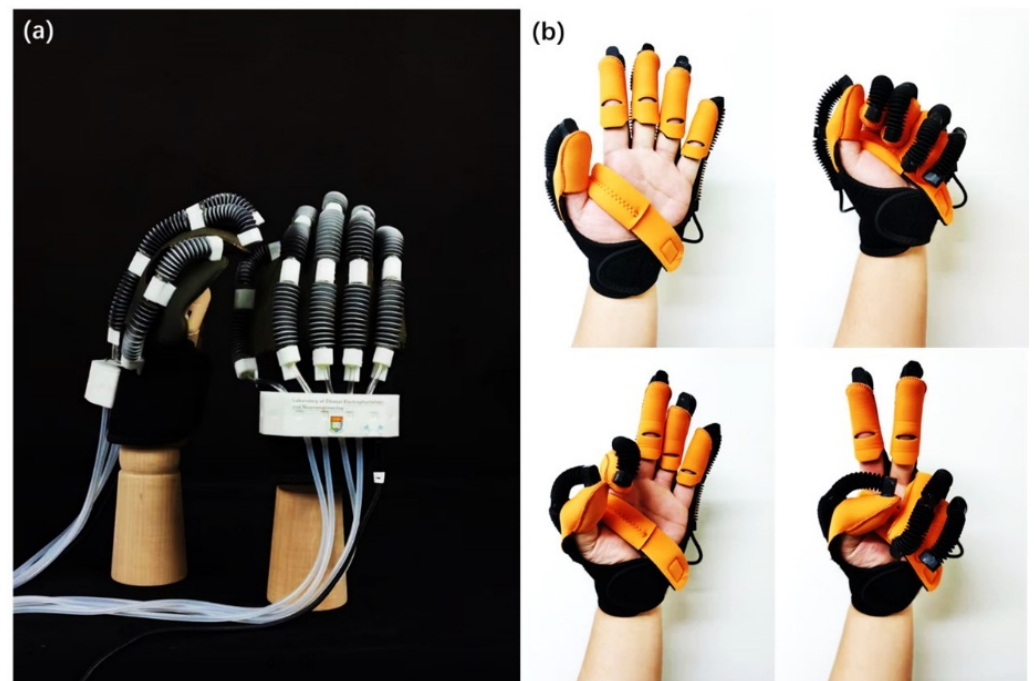


Figure 9. (a) Soft robotic exoskeleton gloves actuated by GBBAs (GBBAs Gloves); (b) four representative gestures realized through the five-channel control system.

Compared to other exoskeleton rehabilitation gloves, GBBAs Gloves have a lighter wearing weight and higher peak output force. The characteristics comparisons are listed in Table 3. Benefiting from larger bending angle along the short-axis symmetry plane of the GBBA, this soft exoskeleton glove has a more compact volume and a larger bending range even compared to those with the same driving method.

Table 3. Original design parameters of elliptical GBBAs.

Name	Actuating Methods	Weight (gram)	Output Tension (N)
Hand of Hope	Motors and links	700 g	12 N
Graspy Glove	Motors and cable	250 g	16 N
Gloreha Lite	Cable	80 g	5 N
Rubber Glove	Pneumatic	180 g	36 N
GBBAs Glove	Pneumatic	95 g	25 N

6. Discussion and Conclusions

In this work, we proposed the configuration and processing method of the pneumatic guided bending bellows actuators with an elliptical section, which are applied to drive the flexion and extension of knuckles in the soft wearable exoskeleton system. The high output performance, light weight, and distinct characteristics of bending guided along various symmetry directions of the actuators contribute to the GBBAs Glove to provide sufficient force for the rehabilitation of hand dysfunctional patients with a compact size and lighter weight. At the same time, the five-way air control system enables this soft exoskeleton glove to be controlled by each finger. Thus, therapists can practically design different rehabilitation programs for patients with various hand dysfunctions.

As a novel structural pneumatic soft actuator, the GBBA exhibits many properties that are beneficial to the design of exoskeleton robots. The thin-walled structure made of TPE material enables the GBBAs to have sufficient structural strength and air tightness under the

condition of light weight. The special structures empower GBBAs to generate pulling and thrusting output force of hundreds of times its own weight. Therefore, the soft exoskeleton gloves with the GBBAs as the driving devices can achieve the purposes of lightweight wearability, and enough pulling force against buckling. The elliptical cross-sectional bellows structure of the GBBAs has unique output of bending along the long- or short-axis symmetry, which are not possessed by the traditional circular cross-sectional bellows. The significance of this feature for replacing the circular cross-sectional bellows made of the same material to drive the soft exoskeleton gloves is that when the output force is kept unchanged, that is, the effective area of the pneumatic actuators is the same, the appearance of the wearable soft exoskeleton gloves becomes compact, and the bending angle of fingers also becomes so wide that the hand can make a fist or open completely. The neoprene gloves driven by the GBBAs are used as wearable lightweight pneumatic soft rehabilitation gloves, showing significantly improved wearing comfort as the result of neither the driving actuators nor the wearing part using a rigid unit. The five-channel control system provides the soft exoskeleton gloves the possibilities that repetitive flexion and extension of specific fingers complete the corresponding gestures to achieve the training and stimulating of the target muscles to achieve the rehabilitation of muscles and motor nerves.

This work elaborated on the components, driving methods, and control effects of the soft exoskeleton gloves driven by the GBBAs. The output force and displacement experiments under linear motion and the bending experiments acting on bionic knuckles and fingers are also included in the work. It is demonstrated by the experiment results of the GBBAs driving the bionic knuckle along two symmetry axes that the elliptical cross-sectional bellows have a larger bending angle along the short-axis plane than the long-axis plane, which has enlightenment for the design of fluidic soft actuators acting on the single-degree-of-freedom rotation joint.

Future works include extending the application of this elliptical cross-sectional bellows structure to the rehabilitation of other similar joints such as elbows; introducing a variety of power modes to the GBBAs such as wire drive and dual drive; and introducing the EEG signal judgement mechanism into the existing soft exoskeleton gloves' control system, combining physical therapy of hand muscles with neurorehabilitation.

Author Contributions: Conceptualization, D.D. and X.L.; methodology, D.D. and Z.W.; software, X.W.; validation, D.D., X.W., and X.L.; formal analysis, D.D.; investigation, Y.H.; resources, Y.H.; data curation, X.W.; writing—original draft preparation, D.D.; writing—review and editing, Y.H.; visualization, D.D.; supervision, Y.H.; project administration, Y.H.; funding acquisition, Y.H. All authors have read and agreed to the published version of the manuscript.

Funding: National Key Research and Development Program of China (2021YFF0501600); Shen-zhen-Hong Kong-Macau Technology Research Programme (Type C. SGDX2019081623201196); Shenzhen Local Science and Technology Development Fund guided by the Chinese Central Government (2021Szvup130).

Data Availability Statement: The data presented in this study are available in this article.

Conflicts of Interest: The authors declare no conflict of interest.

References

1. Cederlund, R.I.; Thomsen, N.; Thrainsdottir, S.; Eriksson, K.-F.; Sundkvist, G.; Dahlin, L.B. Hand disorders, hand function, and activities of daily living in elderly men with type 2 diabetes. *J. Diabetes Its Complicat.* **2009**, *23*, 32–39. [[CrossRef](#)] [[PubMed](#)]
2. Kitago, T.; Goldsmith, J.; Harran, M.; Kane, L.; Berard, J.; Huang, S.; Ryan, S.L.; Mazzoni, P.; Krakauer, J.W.; Huang, V.S. Robotic therapy for chronic stroke: General recovery of impairment or improved task-specific skill? *J. Neurophysiol.* **2015**, *114*, 1885–1894. [[CrossRef](#)] [[PubMed](#)]
3. Ito, S.; Ueki, S.; Ishihara, K.; Miura, M.; Kawasaki, H.; Ishigure, Y.; Nishimoto, Y. Parallel controller construction for a multi-DOF hand rehabilitation equipment. *Int. J. Appl. Electromagn. Mech.* **2011**, *36*, 151–158. [[CrossRef](#)]
4. Casas, R.; Sandison, M.; Chen, T.; Lum, P.S. Clinical Test of a Wearable, High DOF, Spring Powered Hand Exoskeleton (HandSOME II). *IEEE Trans. Neural Syst. Rehabil. Eng.* **2021**, *29*, 1877–1885. [[CrossRef](#)]

5. Metzger, J.-C.; Lambercy, O.; Califfi, A.; Dinacci, D.; Petrillo, C.; Rossi, P.; Conti, F.M.; Gassert, R. Assessment-driven selection and adaptation of exercise difficulty in robot-assisted therapy: A pilot study with a hand rehabilitation robot. *J. Neuroeng. Rehabil.* **2014**, *11*, 154. [[CrossRef](#)]
6. Lambercy, O.; Dovat, L.; Gassert, R.; Burdet, E.; Teo, C.L.; Milner, T. A Haptic Knob for Rehabilitation of Hand Function. *IEEE Trans. Neural Syst. Rehabil. Eng.* **2007**, *15*, 356–366. [[CrossRef](#)] [[PubMed](#)]
7. Hu, X.L.; Tong, K.Y.; Wei, X.J.; Rong, W.; Susanto, E.A.; Ho, S.K. The effects of post-stroke upper-limb training with an electromyography (EMG)-driven hand robot. *J. Electromyogr. Kinesiol.* **2013**, *23*, 1065–1074. [[CrossRef](#)]
8. Laske, E.A.; Davis, D.R.; Bridgwater, L.B.; Ensley, K.G.; Diftler, M.; Linn, D.M.; Ihrke, C.A.; Lee, J.H. RoboGlove-A Robonaut Derived Multipurpose Assistive Device. In Proceedings of the International Conference on Robotics and Automation (No. JSC-CN-30211 2014.), Hong Kong, China, 31 May 2014.
9. Popov, D.; Gaponov, I.; Jee-Hwan, R. Portable Exoskeleton Glove With Soft Structure for Hand Assistance in Activities of Daily Living. *IEEE/ASME Trans. Mechatron.* **2016**, *22*, 865–875. [[CrossRef](#)]
10. Florez, J.M.; Shah, M.; Moraud, E.M.; Wurth, S.; Baud, L.; Von Zitzewitz, J.; van den Brand, R.; Micera, S.; Courtine, G.; Paik, J. Rehabilitative Soft Exoskeleton for Rodents. *IEEE Trans. Neural Syst. Rehabil. Eng.* **2016**, *25*, 107–118. [[CrossRef](#)]
11. Polygerinos, P.; Correll, N.; Morin, S.A.; Mosadegh, B.; Onal, C.D.; Petersen, K.; Cianchetti, M.; Tolley, M.T.; Shepherd, R.F. Soft Robotics: Review of Fluid—Driven Intrinsically Soft Devices. Manufacturing, Sensing, Control, and Applications in Human-Robot Interaction. *Adv. Eng. Mater.* **2017**, *19*, 1700016. [[CrossRef](#)]
12. Siyi Intelligence. Available online: <https://www.siyizn.com/EN.html> (accessed on 24 November 2022).
13. AIREHA. Available online: <https://lap-atom.co.jp/.en/product/> (accessed on 24 November 2022).
14. Pagoli, A.; Chapelle, F.; Corrales-Ramon, J.-A.; Mezouar, Y.; Lapusta, Y. Review of soft fluidic actuators: Classification and materials modeling analysis. *Smart Mater. Struct.* **2021**, *31*, 013001. [[CrossRef](#)]
15. Jung, W.; Kang, Y.; Han, S.; Hwang, Y. Biocompatible micro, soft bellow actuator rapidly manufactured using 3D-printed soluble mold. *J. Micromech. Microeng.* **2019**, *29*, 125005. [[CrossRef](#)]
16. Herianto; Irawan, W.; Ritonga, A.S.; Prastowo, A. Design and fabrication in the loop of soft pneumatic actuators using fused deposition modelling. *Sens. Actuators A Phys.* **2019**, *298*, 111556. [[CrossRef](#)]
17. Tawk, C.; Alici, G. A Review of 3D-Printable Soft Pneumatic Actuators and Sensors: Research Challenges and Opportunities. *Adv. Intell. Syst.* **2021**, *3*, 2000223. [[CrossRef](#)]
18. Guo, N.; Sun, Z.; Wang, X.; Yeung, E.H.K.; To, M.K.T.; Li, X.; Hu, Y. Simulation analysis for optimal design of pneumatic bellow actuators for soft-robotic glove. *Biocybern. Biomed. Eng.* **2020**, *40*, 1359–1368. [[CrossRef](#)]
19. Liu, S.; Fang, Z.; Liu, J.; Tang, K.; Luo, J.; Yi, J.; Hu, X.; Wang, Z. A Compact Soft Robotic Wrist Brace With Origami Actuators. *Front. Robot. AI* **2021**, *8*, 614623. [[CrossRef](#)]
20. Abbasi, P.; Nekoui, M.A.; Zareinejad, M.; Abbasi, P.; Azhang, Z. Position and Force Control of a Soft Pneumatic Actuator. *Soft Robot.* **2020**, *7*, 55–563. [[CrossRef](#)]
21. Felt, W. Folded-Tube Soft Pneumatic Actuators for Bending. *Soft Robot.* **2019**, *6*, 174–183. [[CrossRef](#)]
22. Singh, N.; Saini, M.; Anand, S.; Kumar, N.; Srivastava, M.V.P.; Mehndiratta, A. Robotic Exoskeleton for Wrist and Fingers Joint in Post-Stroke Neuro-Rehabilitation for Low-Resource Settings. *IEEE Trans. Neural Syst. Rehabil. Eng.* **2019**, *27*, 2369–2377. [[CrossRef](#)]
23. Pu, S.-W.; Pei, Y.-C.; Chang, J.-Y. Decoupling Finger Joint Motion in an Exoskeletal Hand: A Design for Robot-Assisted Rehabilitation. *IEEE Trans. Ind. Electron.* **2020**, *67*, 686–697. [[CrossRef](#)]
24. Shiota, K.; Kokubu, S.; Tarvainen, T.V.J.; Sekine, M.; Kita, K.; Huang, S.Y.; Yu, W. Enhanced Kapandji test evaluation of a soft robotic thumb rehabilitation device by developing a fiber-reinforced elastomer-actuator based 5-digit assist system. *Robot. Auton. Syst.* **2019**, *111*, 20–30. [[CrossRef](#)]
25. Elgeneidy, K.; Lohse, N.; Jackson, M. Bending angle prediction and control of soft pneumatic actuators with embedded flex sensors—A data-driven approach. *Mechatronics* **2018**, *50*, 234–247. [[CrossRef](#)]
26. Tang, Z.Q.; Heung, H.L.; Shi, X.Q.; Tong, R.K.Y.; Li, Z. Probabilistic Model-Based Learning Control of a Soft Pneumatic Glove for Hand Rehabilitation. *IEEE Trans. Biomed. Eng.* **2022**, *69*, 1016–1028. [[CrossRef](#)] [[PubMed](#)]
27. Guo, L.; Li, K.; Cheng, G.; Zhang, Z.; Xu, C.; Ding, J. Design and Experiments of Pneumatic Soft Actuators. *Robotica* **2021**, *39*, 1806–1815. [[CrossRef](#)]
28. Sun, E.; Wang, T.; Zhu, S. An experimental study of bellows-type fluidic soft bending actuators under external water pressure. *Smart Mater. Struct.* **2020**, *29*, 87005. [[CrossRef](#)]
29. Bishop-Moser, J.; Kota, S. Design and Modeling of Generalized Fiber-Reinforced Pneumatic Soft Actuators. *IEEE Trans. Robot.* **2015**, *31*, 536–545. [[CrossRef](#)]
30. Virgala, I.; Kelemen, M.; Varga, M.; Kurylo, P. Analyzing, Modeling and Simulation of Humanoid Robot Hand Motion. *Procedia Eng.* **2014**, *96*, 489–499. [[CrossRef](#)]
31. Wang, H.; Chen, P.; Li, Y.; Sun, B.; Liao, Z.; Niu, B.; Niu, J. New Rehabilitation Assessment Method of the End-Effector Finger Rehabilitation Robot Based on Multi-Sensor Source. *Healthcare* **2021**, *9*, 1251. [[CrossRef](#)]
32. Cerveri, P.; De Momi, E.; Lopomo, N.; Baud-Bovy, G.; Barros, R.M.L.; Ferrigno, G. Finger kinematic modeling and real-time hand motion estimation. *Ann. Biomed. Eng.* **2007**, *35*, 1989–2002. [[CrossRef](#)]
33. Wang, J.; Liu, Z.; Fei, Y. Design and Testing of a Soft Rehabilitation Glove Integrating Finger and Wrist Function. *J. Mech. Robot.* **2019**, *11*, 011015. [[CrossRef](#)]

34. Wang, X.; Cheng, Y.; Zheng, H.; Li, Y.; Wang, C. Design and optimization of actuator for multi-joint soft rehabilitation glove. *Ind. Robot.* **2021**, *48*, 877–890. [[CrossRef](#)]
35. Thalia, D.P.; Risangtuni, A.G. PID control for soft actuator pneumatic glove. In *AIP Conference Proceedings*; AIP Publishing LLC: Melville, NY, USA, 2019.
36. Yue, Z.; Zhang, X.; Wang, J. Hand Rehabilitation Robotics on Poststroke Motor Recovery. *Behav. Neurol.* **2017**, *2017*, 3908120–3908135. [[CrossRef](#)] [[PubMed](#)]